Please cite this article in press as: Ghazizadeh et al., Prospective Isolation of ISL1+ Cardiac Progenitors from Human ESCs for Myocardial Infarction Therapy, Stem Cell Reports (2018), https://doi.org/10.1016/j.stemcr.2018.01.037

Stem Cell Reports
Article

ISSCR

OPEN ACCESS

Prospective Isolation of ISL1$^+$ Cardiac Progenitors from Human ESCs for Myocardial Infarction Therapy

Zaniar Ghazizadeh,[1,2,13,*] Faranak Fattahi,[3,13,14] Mehdi Mirzaei,[4,5,6] Delger Bayersaikhan,[7] Jaesuk Lee,[7] Sehyun Chae,[8] Daehee Hwang,[8] Kyunghee Byun,[7] Mehdi Sharifi Tabar,[3] Sara Taleahmad,[3] Shahab Mirshahvaladi,[3] Parisa Shabani,[1] Hananeh Fonoudi,[1] Paul A. Haynes,[4] Hossein Baharvand,[1,9] Nasser Aghdami,[1,10] Todd Evans,[11] Bonghee Lee,[7,*] and Ghasem Hosseini Salekdeh[3,12,*]

[1]Department of Stem Cells and Developmental Biology, Cell Science Research Center, Royan Institute for Stem Cell Biology and Technology, ACECR, Tehran, Iran
[2]School of Medicine, Tehran University of Medical Sciences, Tehran, Iran
[3]Department of Molecular Systems Biology, Cell Science Research Center, Royan Institute for Stem Cell Biology and Technology, ACECR, Banihashem Square, Banihashem Street, Ressalat Highway, Tehran, Iran
[4]Department of Chemistry and Biomolecular Sciences, Macquarie University, Sydney, NSW, Australia
[5]Faculty of Medicine and Health Sciences, Macquarie University, Sydney, NSW, Australia
[6]Australian Proteome Analysis Facility, Macquarie University, Sydney, NSW, Australia
[7]Center for Regenerative Medicine, Gachon University, Incheon City, Republic of Korea
[8]Department of New Biology and Center for Plant Aging Research, Institute for Basic Science, Daegu Gyeongbuk Institute of Science and Technology, Daegu, Republic of Korea
[9]Department of Developmental Biology, University of Science and Culture, ACECR, Tehran, Iran
[10]Department of Regenerative Biomedicine at Cell Science Research, Royan Institute for Stem Cell Biology and Technology, ACECR, Tehran, Iran
[11]Department of Surgery, Weill Cornell Medicine, New York, NY, USA
[12]Department of Molecular Sciences, Macquarie University, Sydney, NSW, Australia
[13]Co-first author
[14]Present address: Department of Biochemistry and Biophysics, Eli and Edythe Broad Center of Regeneration Medicine and Stem Cell Research, School of Medicine, University of California, San Francisco.
*Correspondence: zghazizadeh@bwh.harvard.edu (Z.G.), bhlee@gachon.ac.kr (B.L.), salekdeh@royaninstitute.org (G.H.S.)
https://doi.org/10.1016/j.stemcr.2018.01.037

SUMMARY

The LIM-homeodomain transcription factor ISL1 marks multipotent cardiac progenitors that give rise to cardiac muscle, endothelium, and smooth muscle cells. ISL1$^+$ progenitors can be derived from human pluripotent stem cells, but the inability to efficiently isolate pure populations has limited their characterization. Using a genetic selection strategy, we were able to highly enrich ISL1$^+$ cells derived from human embryonic stem cells. Comparative quantitative proteomic analysis of enriched ISL1$^+$ cells identified ALCAM (CD166) as a surface marker that enabled the isolation of ISL1$^+$ progenitor cells. ALCAM$^+$/ISL1$^+$ progenitors are multipotent and differentiate into cardiomyocytes, endothelial cells, and smooth muscle cells. Transplantation of ALCAM$^+$ progenitors enhances tissue recovery, restores cardiac function, and improves angiogenesis through activation of AKT-MAPK signaling in a rat model of myocardial infarction, based on cardiac MRI and histology. Our study establishes an efficient method for scalable purification of human ISL1$^+$ cardiac precursor cells for therapeutic applications.

INTRODUCTION

The LIM-homeodomain transcription factor ISL1 marks an SHF (second heart field) progenitor population that makes a substantial contribution to the developing heart after the initial heart tube formation, giving rise to most cells in the right ventricle, pacemaker cells, both atria, the outflow tract, and specific regions of the left ventricle (Buckingham et al., 2005; Cai et al., 2003; Laugwitz et al., 2005; Liang et al., 2015; Wu et al., 2008). The ISL1$^+$ progenitors also differentiate into smooth muscle cells and endothelial cells (Bu et al., 2009; Sun et al., 2007).

Despite their significant contribution to the heart, there is less known about their developmental and regenerative potential in humans due to limitations in obtaining these embryonic cells from primary samples. Human pluripotent stem cells (hPSCs) offer a renewable source for obtaining, in principle, unlimited numbers of ISL1$^+$ cardiac progenitors. However, currently available differentiation protocols yield highly heterogeneous populations that complicate disease modeling, drug screening, and regenerative applications.

Several groups have previously shown that a transient ISL1$^+$ progenitor population emerges at early stages during cardiac differentiation of hPSCs (Bu et al., 2009). Although these progenitors are thought to subsequently give rise to beating cardiomyocytes, their differentiation potency and molecular characteristics have remained elusive due to the heterogeneity of the hPSC-derived cultures and lack of a faithful reporter or surface marker to facilitate purification. Moreover, surface markers that have been identified label either later stage cardiac cells, e.g., SIRPA (Dubois et al., 2011), or earlier mesodermal committed cells (Drukker et al., 2012). Since ISL1 is a nuclear transcription factor, it cannot be used directly for purification of ISL1$^+$ cells.

Please cite this article in press as: Ghazizadeh et al., Prospective Isolation of ISL1+ Cardiac Progenitors from Human ESCs for Myocardial Infarction Therapy, Stem Cell Reports (2018), https://doi.org/10.1016/j.stemcr.2018.01.037

However, we reasoned that the ISL1 promoter could be used to drive expression of a reporter gene that accurately identifies ISL1-expressing cells.

We then used comparative quantitative proteomics to search for surface markers that specifically label the ISL1+ cardiac progenitor cells derived from hPSCs. We identified ALCAM (CD166) as a specific surface marker that can be used to enrich for these progenitor cells. We further used this purification strategy to characterize the human ISL1+ cardiac progenitors and demonstrated their potential for cell therapy in a myocardial infarction model.

RESULTS

Purification and Molecular Characterization of ISL1+ Cardiac Progenitors

To facilitate purification and characterization of hPSC-ISL1+ progenitors, we established a human embryonic stem cell (hESC) line expressing the hygromycin resistance gene under control of the ISL1 promoter (Figure S1A). The modified hESCs (rH5-ISL1-Hygro) express the key pluripotency genes TRA1-60, TRA1-81, OCT4, and NANOG (Figure S1B), indicating that the genetic modification and clonal selection did not alter their pluripotent phenotype. To generate cardiac progenitor cells from the modified hESCs, we used a modified version of the protocol described by Laflamme et al. (2007) (Figure 1A), which involves an initial replating step 5 days before treatment with activin A and bone morphogenetic protein 4 (BMP4). Five days after differentiation, cells significantly increased the expression of ISL1 gene. Given that ISL1 expression increases progressively between day 5 and day 10 of differentiation (Figures 1B and S1C), we treated the rH5-ISL1-Hygro cells from day 5 through day 8 with hygromycin to select for the hESC-derived ISL1+ cells (Figure 1C). The hygromycin selection enriches for ISL1+ cells, yielding a population of about 90% positive for ISL1 as assessed by immunofluorescence staining, flow cytometry (Figure 1D), and western blotting experiments (Figure S1D). The ISL1-enriched cell population also expresses relatively higher levels of cardiac mesoderm transcription factors *NKX2.5*, *GATA4*, and *MEF2C* (Figure S1E), the latter of which is transcriptionally regulated by ISL1 (Dodou et al., 2004). We maintained differentiated cells for up to 25 days to evaluate the expression pattern of structural proteins and functional characterization of ISL1-enriched cells. The hygromycin selected cells differentiate into cardiomyocytes expressing CX43, MYH6, and cardiac troponin T (Figure S1F), and generate beating cardiomyocytes (Movie S1 and Figure S1F). Multi-electrode array (MEA) analysis shows that the spontaneous beating cardiomyocytes increase their beating rate in response to isoproterenaline treatment, indicating functional maturation (Figures S1G and S1H).

A Mass Spectrometry Approach Identifies ALCAM as ISL1+ Cardiac Progenitor Surface Marker

To further characterize the hESC-derived ISL1+ progenitors and identify surface markers to facilitate their prospective isolation, we performed an unbiased global proteomics analysis. We performed a label-free quantitative shotgun proteomics assay using a spectral counting approach to compare the ISL1+-enriched population with nonenriched age-matched differentiated cells. The hierarchical clustering and list of the differentially expressed proteins is presented in Figure S2A and Table S1. The key differentially expressed pathways following ISL1 enrichment revealed by Qiagen Ingenuity Pathway Analysis were associated with transcriptional regulators, signaling pathway regulators (including modulators of WNT and Notch pathways), cardiovascular development proteins, and cardiovascular disease-related proteins (Figures S2B–S2E).

Focusing on surface markers that were differentially expressed in the ISL1+ enriched and unenriched populations, we identified CD49C and CD276 as potential negative markers and ALCAM (CD166) as a candidate positive marker (Figure 1E). Western blotting analysis for selected differentially expressed surface antigens confirmed the global proteomics results (Figure S2F). Immunofluorescence staining on ISL1+-enriched and unenriched populations, as well as sorted populations, showed that ALCAM specifically labels the hESC-derived ISL1+ progenitors (Figures 2A–2D) while negative sorts for CD49C or CD276 did not result in a significant enrichment (Figures S2G and S2H). Immunofluorescence staining confirms co-expression of ISL1 and MEF2C with ALCAM in hESC-derived cardiac progenitors (Figure 2E), indicating that ALCAM faithfully labels ISL1+ progenitors derived from hESCs.

Time-course gene expression analysis of the hESC-derived cells by qRT-PCR and flow cytometry reveals that ALCAM is upregulated at day 8 and maintained in later stages of differentiation (Figures 2D and 2E). The hESC-derived ALCAM-sorted cells are multipotent and can be further differentiated into cardiomyocytes expressing MYH6, CX43, MLC-2v, c-Actin, SMA+ smooth muscle precursors, and VE-cadherin+ endothelial cells (Figures 2F, 2G, and S3A). Persistent expression of ALCAM is also confirmed by flow cytometry at different time points in differentiating hESCs and human induced PSCs (hiPSCs) (Figures S3B and S3C).

We then compared the expression pattern of ALCAM with other previously identified surface markers for various hPSC-derived cardiac populations. At day 8, when we expected to see a high percentage of ISL1+ progenitors in the population, we did not observe a substantial number

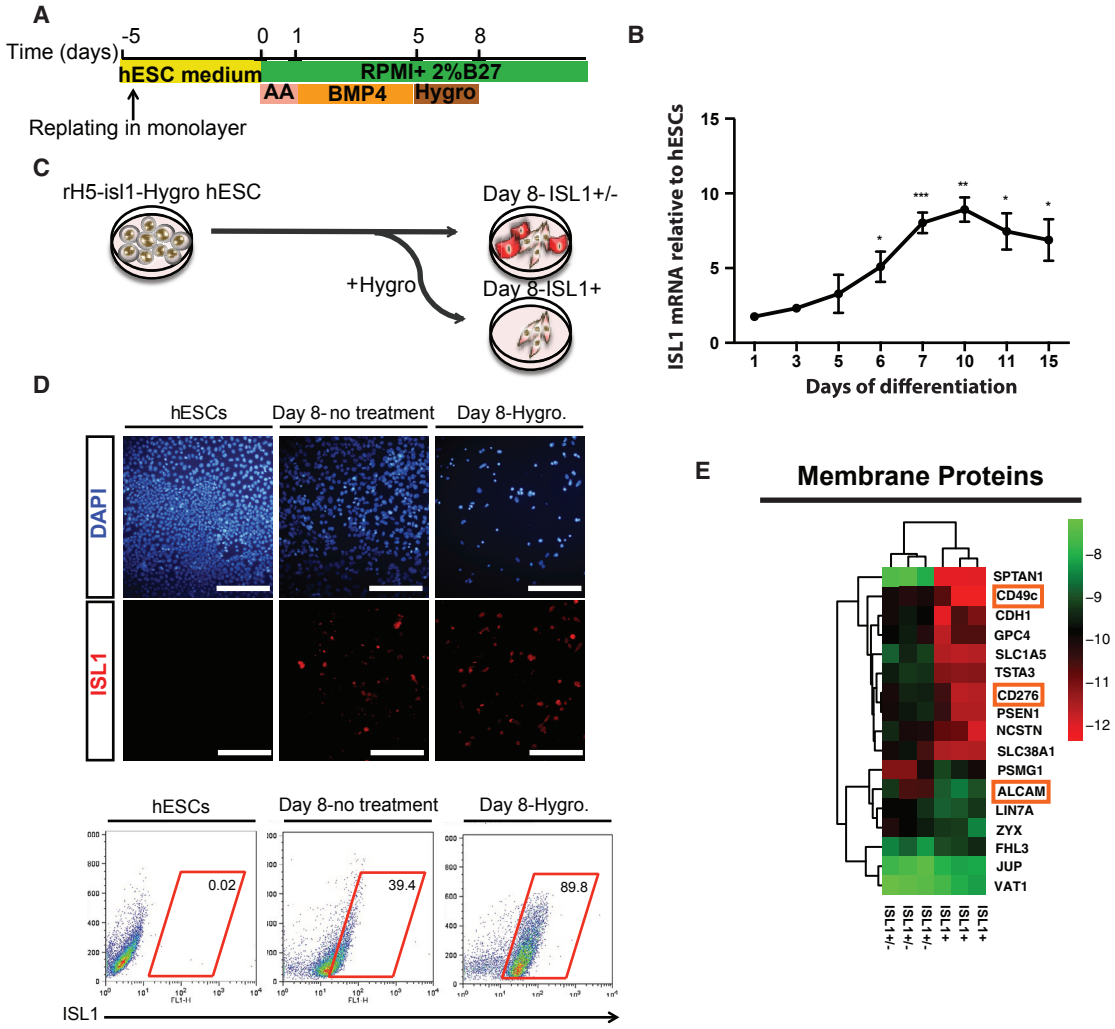

Figure 1. Enrichment and Proteomic Characterization of hESC-Derived ISL1+ Progenitors

(A) Schematic representation of the differentiation protocol.

(B) Real-time qRT-PCR for *ISL1* expression during cardiac differentiation of rH5-isl1-Hygro. n = 3.

(C) Antibiotic treatment paradigm for enrichment of ISL1+ cells.

(D) Immunofluorescence staining and flow cytometry of hESCs at day 8 of differentiation with or without antibiotic treatment for ISL1.

(E) Membrane proteins that were ≥1.5-fold differentially expressed (n = 3 independent experiments) between antibiotic-treated cells versus untreated cells. AA, activin A.

Data are mean ± SEM. *p < 0.05, **p < 0.01, ***p < 0.001. Scale bar, 75 μm.

of SIRPA-, VCAM-, or CD13-expressing cells, while the percentage of PDGFRα- and SSEA-1-positive cells were relatively high and the majority also expressed ALCAM (Figure S3D).

SIRPA, a recently defined cardiomyocyte precursor marker (Dubois et al., 2011), is upregulated after the window of ISL1 expression and is reduced in the differentiated population, indicating that the two markers label temporally or developmentally distinct precursor populations (Figure S3E). Taken together, these data confirm that purification of ALCAM+ cells is a reliable approach for obtaining ISL1+ multipotent cardiac progenitors from differentiating hPSCs.

ALCAM-Sorted Cells Exhibit a Gene Expression Pattern Characteristic of a Proliferative State

We next performed gene expression profiling for ALCAM+, ALCAM−, and the unsorted age-matched differentiated cells (ALCAM−/+), in comparison with undifferentiated hESCs. We identified 3,366 differentially expressed genes (DEGs) and clustered them based on their expression patterns in different cell populations (Figures 3A and 3B;

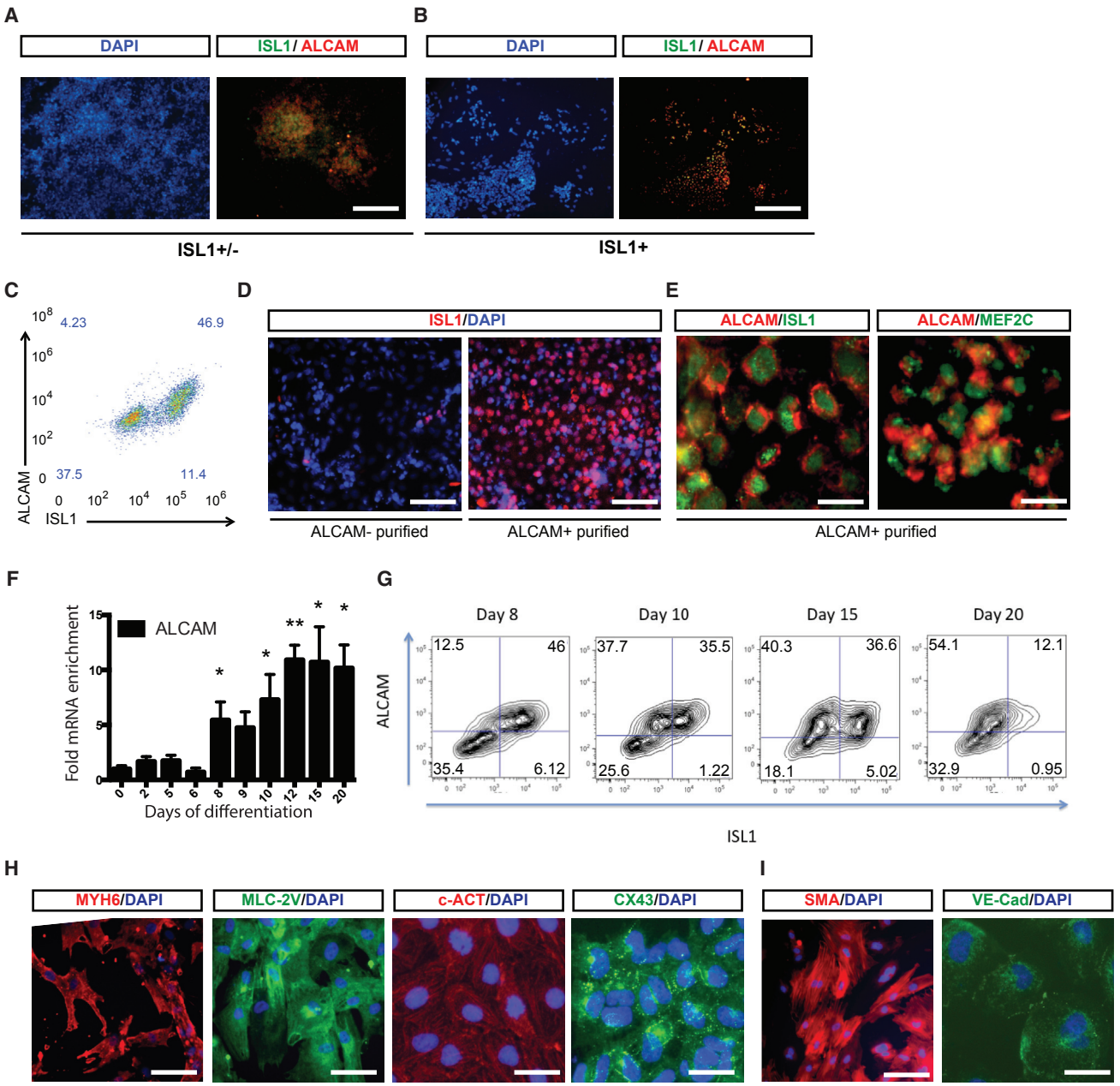

Figure 2. ALCAM Labels Multipotent hESC-Derived ISL1+ Progenitors during Cardiac Differentiation

(A and B) ISL1 and ALCAM staining of (A) ISL1$^{+/-}$ and (B) ISL^{+} populations.

(C) Flow-cytometry analysis for co-expression of ALCAM and ISL1.

(D) ISL1 staining of ALCAM^{-} (left panel) and ALCAM^{+} (right panel) sorted populations.

(E) Immunofluorescent co-staining of ALCAM with ISL1 and MEf2C in differentiated cells.

(F) Time-course qPCR analysis of *ALCAM* mRNA expression. n = 3–5 independent experiments. *p < 0.05, **p < 0.01.

(G) Time-course flow-cytometry analysis for co-expression of ALCAM and ISL1. The cells were sorted at day 8 for ALCAM for subsequent characterizations.

(H) Immunolabeling for MYH6, MLC-2v, c-Actin, and CX43 in ALCAM^{+} sorted populations differentiated toward cardiomyocyte lineage.

(I) Immunolabeling for SMA and VE-cadherin in ALCAM^{+} sorted populations differentiated toward smooth muscle and endothelial lineages, respectively.

Scale bars, 100 μm (A and B), 50 μm (D), 10 μm (E, H, and I [right panel]), and 20 μm (I [left panel]).

Please cite this article in press as: Ghazizadeh et al., Prospective Isolation of ISL1+ Cardiac Progenitors from Human ESCs for Myocardial Infarction Therapy, Stem Cell Reports (2018), https://doi.org/10.1016/j.stemcr.2018.01.037

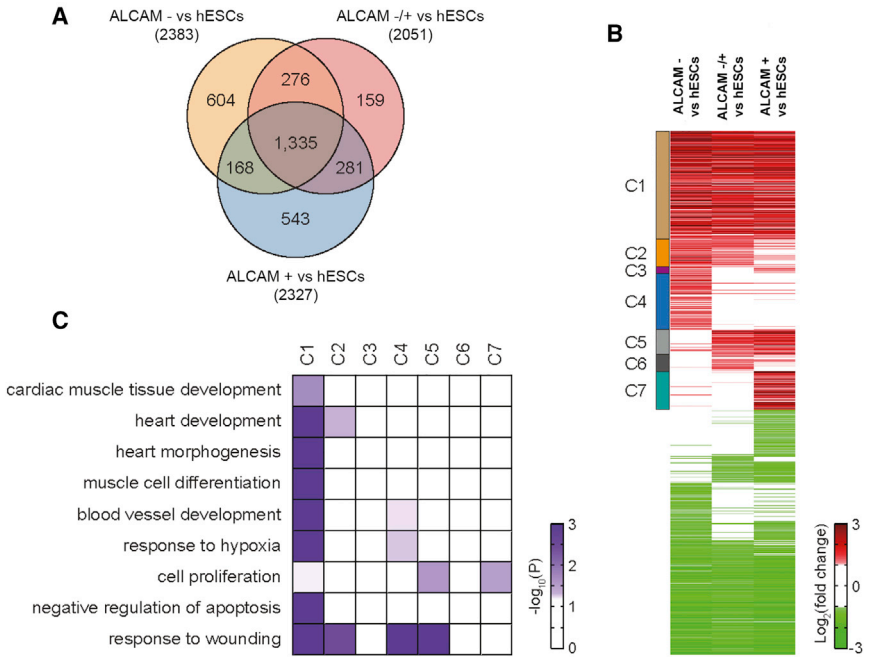

Figure 3. Upregulation of Proliferation Pathways in ALCAM+ Cells

(A) Venn diagram for differentially expressed genes (DEGs) in ALCAM^{-}, ALCAM$^{-/+}$, and ALCAM^{+} cells versus hESCs.

(B) Heatmap representing the differential expression of the genes in the 14 clusters with distinct expression patterns across the populations (see Table S2 for the list of genes in each cluster). The color bar represents the gradient of $\log_2$ fold changes between the two types of cells indicated in each column.

(C) Gene ontology and biological processes enriched in clusters 1 to 7 (C1–C7). The color bar represents the gradient of $-\log_{10}(P)$ where P is the significance of individual GOBPs being enriched by the DEGs.

Table S2). We focused on seven cluster transcripts that were upregulated in all samples versus hESCs (clusters 1–7, Figure 3B), to identify cellular processes that are activated upon differentiation and purification of ALCAM^{+} progenitors. Enrichment analysis of gene ontology biological processes for clusters shows that the genes in cluster 1, which are upregulated in all three types of cells (ALCAM^{-}, ALCAM$^{-/+}$, and ALCAM^{+} cells) compared with hESCs, are mainly involved in the processes related to cardiac differentiation (cardiac muscle tissue development, heart development, heart morphogenesis, and muscle cell differentiation), angiogenesis (blood vessel development and response to hypoxia), and anti-apoptosis (negative regulation of apoptosis; Figure 3C). The genes that regulate cell proliferation are significantly enriched in ALCAM^{+} purified cells (clusters 5 and 7, Figure 3C), suggesting that they are in a progenitor state and may have better regenerative potential in cardiac infarction models.

Improvement of Cardiac Function after Transplantation of ALCAM^{+} Cells in an *In Vivo* Model of Myocardial Infarction

To assess the ability of ALCAM^{+} purified progenitors to improve cardiac function *in vivo*, we used a rat left anterior descending artery (LAD) ligation model of cardiac infarction. The ALCAM^{-}, ALCAM$^{-/+}$ and ALCAM^{+} cells were injected into the border zone surrounding the infarct area anteriorly and laterally (5×10^5) in three places (Figure 4A). Post-transplantation survival of the cells at the injection site was confirmed by immunohistochemistry for human-specific marker Hu-Nu. The number of surviving human cells decreased dramatically after 2 weeks with no surviving human cells at 28 days (Figure S4A). Tissue regeneration capacity of the hESC-derived cells was assessed 2 weeks and 4 weeks after acute myocardial infarction (AMI) by measuring the thickness of the left ventricular wall, and size of the fibrotic area using H&E or Masson's trichrome staining (Figures S4B and 4B). The ventricular thickness was increased significantly in animals transplanted with ALCAM^{+} compared with ALCAM^{-}, ALCAM$^{-/+}$, or vehicle control rats (Figures 4B and 4C), demonstrating the beneficial therapeutic effect of the enriched cardiac progenitors. The size of the fibrotic area showed a substantial decrease in all injection groups compared with the vehicle control group, with the ALCAM^{+} group showing the most statistically significant effect (Figures 4B and 4D).

TUNEL staining of transplanted hearts showed that the population of apoptotic cells increased up to about 69% in the control infarcted group but decreased significantly in all cell transplanted animals, most for the group that received ALCAM^{+} precursors (Figures 4E and S4C). The vehicle control group did not show any improvements compared with the control AMI group (Figures 4B–4E).

To assess the ability of ALCAM^{+} cells to improve angiogenesis, we measured the diameter of blood vessels and number of capillaries in the infarct area and border area in all transplanted animals, using α-smooth muscle actin (α-SMA) and von Willebrand factor (vWF) staining to label vascular smooth muscle and endothelial cells, respectively

Please cite this article in press as: Ghazizadeh et al., Prospective Isolation of ISL1+ Cardiac Progenitors from Human ESCs for Myocardial Infarction Therapy, Stem Cell Reports (2018), https://doi.org/10.1016/j.stemcr.2018.01.037

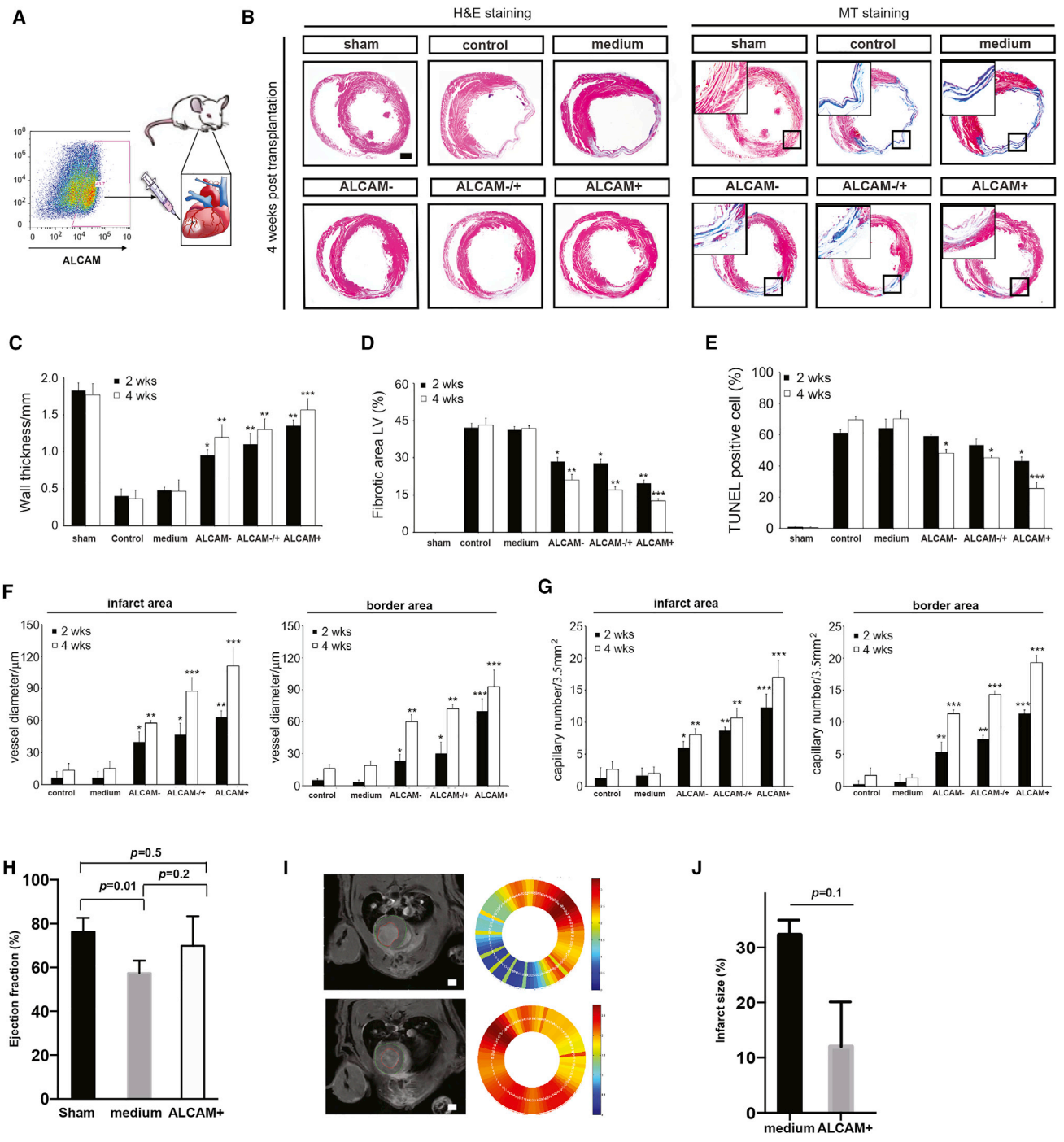

Figure 4. ALCAM$^+$ Cells Promote Tissue Regeneration and Angiogenesis in AMI Rat Hearts

(A) Paradigm for purification and transplantation of ALCAM$^+$ progenitors.

(B and C) H&E staining and Masson's trichrome (MT) staining in sham or AMI rat hearts in control, medium only, and ALCAM$^-$, ALCAM$^{-/+}$, or ALCAM$^+$ cell transplanted groups, 4 weeks post transplantation. Insets are high-magnification images of the fibrotic area. Scale bar, 1 mm.

(C) Wall thickness in transplanted hearts measured by H&E staining.

(D) Fibrotic area in transplanted hearts measured by MT staining.

(E) Quantification of TUNEL staining in sham or AMI rat hearts in control, medium only, and ALCAM$^-$, ALCAM$^{-/+}$, or ALCAM$^+$ cell transplanted groups, 2 and 4 weeks post transplantation.

(legend continued on next page)

(Figures S4D–S4G). In both evaluated regions, the increase in the diameter of the blood vessels was significantly higher in ALCAM$^+$ cell transplanted groups compared with the ALCAM$^{+/-}$, ALCAM$^-$, and control groups (Figure 4F). ALCAM$^+$ transplanted hearts also showed the greatest increase in number of capillaries in 4 weeks compared with other groups (Figure 4G). Taken together, these results show that hESC-derived ALCAM$^+$ cells enhance angiogenesis in AMI rats and have a higher regenerative potential compared with ALCAM$^{+/-}$ and ALCAM$^-$cells.

Given the significant impact of transplanted hESC-derived ALCAM$^+$ cells on overall tissue regeneration in AMI hearts, we set out to evaluate their effects on functional restoration using magnetic resonance imaging (MRI). We observed a profound recovery in hearts that were injected with ALCAM$^+$ cells (Figure S5 and Movie S2). Ejection fraction in the medium-injected rats was significantly lower than in the sham-operated rats (no myocardial infarction) but there was no significant difference between ALCAM$^+$ cell transplanted hearts and sham-operated rats (Figure 4H). This finding confirms a remarkable ability of ALCAM$^+$ cells in almost complete restoration of ventricular function back to normal (n = 3). In addition, preliminary studies showed a trend toward improved wall thickness (Figure 4I) and infarct size (Figure 4J) in ALCAM$^+$ transplanted hearts versus the medium-treated hearts as measured by cardiac MRI imaging. These results demonstrate the potential of ALCAM$^+$ hESC-derived cardiac progenitors for cell therapy in myocardial infarction.

ALCAM$^+$ Purified Progenitors Increase Angiogenesis through Activation of MAPK/ERK, AKT, and JNK Pathways

It is known that angiogenesis can be stimulated through activation of MAPK and AKT pathways (Zhu et al., 2002). To understand the mechanism through which the transplanted ALCAM$^+$ cells improve angiogenesis, we monitored control and transplanted hearts 4 weeks after injection, and measured changes in the levels of AKT, pAKT, ERK1/2, pERK1/2, SAPK/JNK, and pSAPK/JNK (Figure 5A). The levels of AKT, ERK, and SAPK/JNK were similarly increased in all cell treatment groups. However, the phosphorylated active forms of these signaling molecules, pAKT (Figure 5B), pERK1/2 (Figure 5C), and pSAPK/JNK (Figure 5D), were increased most significantly in the ALCAM$^+$ transplanted group, indicating higher activity of these angiogenic factors in ALCAM$^+$ cells. Taken together, these data confirm the superior regenerative potential of ALCAM$^+$-enriched progenitor cells compared with unenriched populations.

DISCUSSION

hPSCs offer a renewable source of cardiac lineages for basic and translational investigations. However, currently available differentiation protocols yield heterogeneous populations that limit their utilization in regenerative medicine. There have been previous attempts to establish surface marker-based methods for purification of cardiomyocyte precursors at various stages of *in vitro* differentiation (Ardehali et al., 2013; Dubois et al., 2011). SIRPA, KDR/PDGFRα, and SSEA4 are among the most common markers that have been used for prospective isolation of cardiac lineages on the basis of co-expression with cardiomyocyte specific markers. Our study is focused on a distinct progenitor stage that is labeled by the transcription factor ISL1. During development, ISL1 marks undifferentiated cardiac progenitors that will contribute to the second wave of cardiogenesis (Liang et al., 2015). These precursors give rise to cardiac smooth muscle, endothelium, pacemakers, and a substantial population of cardiomyocytes. We used a genetic selection approach to obtain enriched ISL1$^+$ progenitors from cardiac differentiation cultures derived from hESCs and subjected them to quantitative proteomic characterization. Pathway analysis suggested that proteins involved in WNT and Notch signaling pathways regulate ISL$^+$ cardiac progenitors, confirming previous findings in murine models (Kwon et al., 2009). In addition, several proteins related to cardiac disease and arrhythmias were among the differentially expressed proteins identified, providing useful leads for further studies in disease modeling. Analysis of membrane proteins enriched in the purified ISL1$^+$ population identified ALCAM (CD166) as a surface marker that can be utilized for prospective isolation of these progenitors from

(F) Quantification of vessel diameter by SMA staining in infarct area (left panel) or border area (right panel) in sham or AMI rat hearts in control, medium only, and ALCAM$^-$, ALCAM$^{-/+}$, or ALCAM$^+$ cell transplanted groups, 2 and 4 weeks post transplantation.
(G) Quantification of capillary numbers by vWF staining in infarct area (left panel) or border area (right panel) in sham or AMI rat hearts in control, medium only, and ALCAM$^-$, ALCAM$^{-/+}$, or ALCAM$^+$ cell transplanted groups, 2 and 4 weeks post transplantation.
(H) *In vivo* MRI quantification of ejection fraction in sham, vehicle, and ALCAM$^+$ cell injected AMI hearts.
(I) Representative MRI images showing regions of interest in medium (upper graph) and ALCAM$^+$ AMI (lower graph) rat hearts 4 weeks after transplantation. Scale bars, 0.5 mm.
(J) Infarct size measurements in sham, control, and ALCAM$^+$ cell injected AMI hearts from *in vivo* MRI. n = 3 independent experiments. *p < 0.05, **p < 0.01, ***p < 0.001.

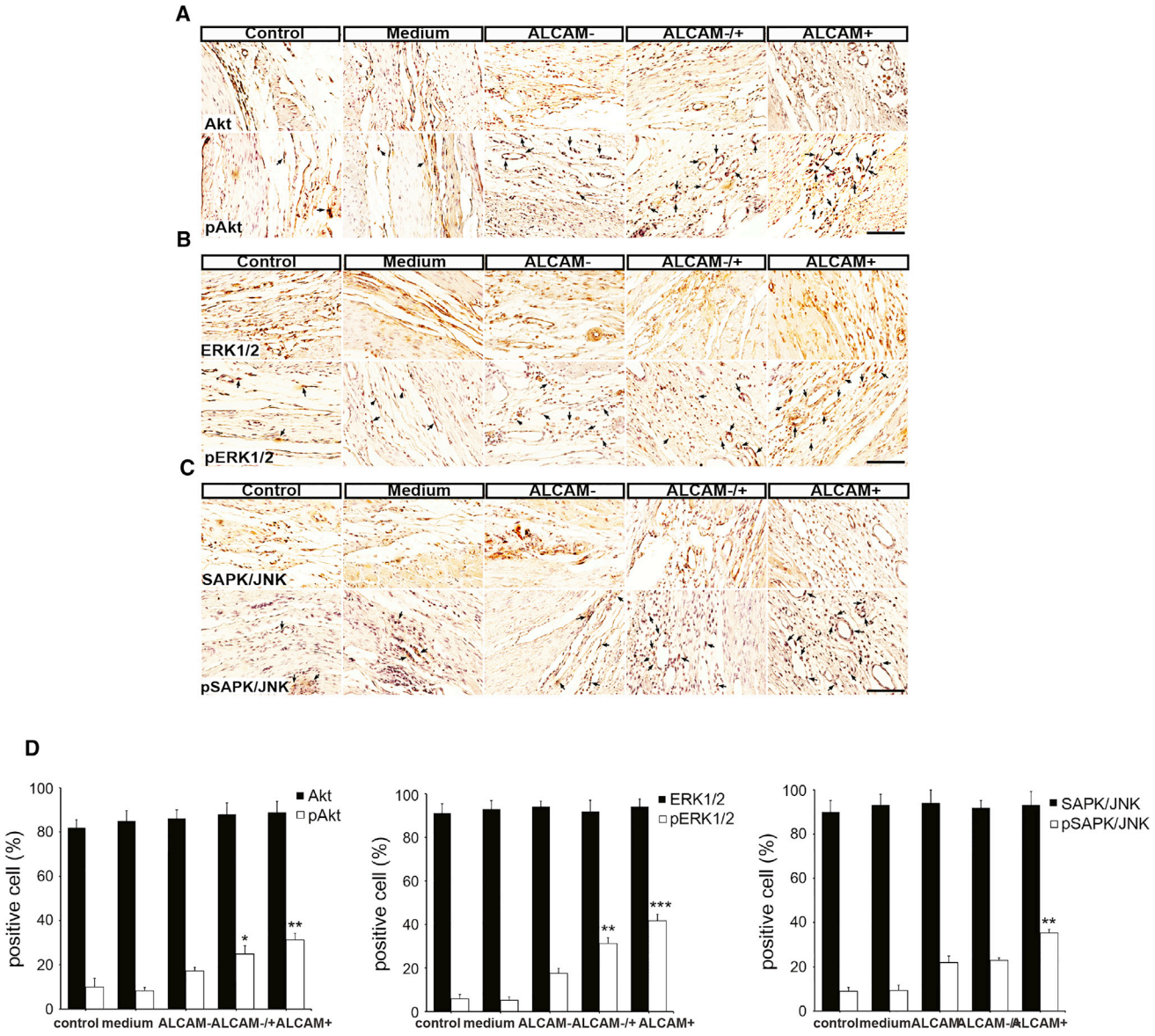

Figure 5. ALCAM+ Cells Promote Angiogenesis in AMI Rat Hearts through AKT, MAPK, and JNK Pathways

(A–C) Immunohistochemistry for Akt, pAkt (A), ERK1/2, pERK1/2 (B), and SAPK/JNK, pSAPK/JNK (C), in AMI rat hearts in control, medium only, and ALCAM^{-}, ALCAM$^{-/+}$, or ALCAM^{+} cell transplanted groups, 4 weeks post transplantation. n = 3 independent experiments. The black arrows point to positive signals. Scale bars, 100 μm.

(D) Quantification of distribution of Akt, pAkt, ERK1/2, pERK1/2, SAPK/JNK, and pSAPK/JNK. *p < 0.05, **p < 0.01, ***p < 0.001.

hPSCs. ALCAM expression exhibits a pattern similar to ISL1 expression at the early stages of differentiation; however, unlike ISL1, it persists through differentiation into mature cardiomyocytes. We also observed that ALCAM has a distinct expression pattern compared with other cardiac surface markers such as SIRPA, which is considered to label more mature cardiomyocytes. Therefore, ALCAM offers a purification strategy for isolation of an earlier and potentially more plastic progenitor population.

ALCAM has been previously shown to mark mature and functional cardiomyocytes and also to mark murine sinoatrial cells, all of which are derivatives of ISL1^{+} cardiac progenitors during development (Liang et al., 2015; Lin et al., 2012; Scavone et al., 2013). An interesting finding of our present study is that ALCAM^{+} cells that are isolated at early stages of differentiation can generate multiple cell types of interest, including functional cardiomyocytes, endothelial cells, and smooth muscle cells. In a recent study, Fernandes

et al. (2015) showed that transplantation of a differentiated population that contains endothelial precursors in addition to cardiomyocytes better improves cardiac function compared with cardiomyocyte committed precursors.

Using a rat model of cardiac infarction, we demonstrated that transplanted ALCAM+ hESC-derived progenitors show a remarkable capacity to promote histological and functional restoration compared with unsorted and ALCAM− cells, suggesting that the enrichment step facilitates optimal tissue regeneration after cell-based treatment. It is possible that by using ALCAM+ cardiac progenitors for transplantation, we could benefit from their potential in differentiating toward smooth muscle and endothelial cells as well as their higher proliferation capacity, as shown by microarray studies. However, the mechanisms by which ALCAM+ cells promote regeneration remains unclear. It is possible that the effect is mediated by secretion of paracrine factors to stimulate endogenous repair or the ability of transplanted cells to promote the formation of functional blood vessels and thereby enhance tissue recovery. It would be interesting to compare the regenerative impact of ALCAM+ cell transplantation with injection of angiogenic factors such as vascular endothelial growth factor to define the role of angiogenesis in the overall repair process.

Furthermore, we showed that the increase in angiogenesis is associated in ALCAM+ grafts with elevated levels of pAKT, a well-known modulator of angiogenesis. One advantage of the current study over previous reports is the application of cardiac MRI for live assessment of heart function after transplantation. We confirmed functional restoration of the infarcted hearts after transplantation of ALCAM+ progenitors. The MRI approach enables a noninvasive, accurate, and direct assessment of heart function in infarcted hearts by measuring infarction area and ejection fraction. However, one of the limitations of the current study was the limited number of animals analyzed by cardiac MRI. To provide a more comprehensive understanding of heart function after transplantation, future studies will involve larger animal cohorts. Moreover, implementation of approaches that increase the survival of progenitors after transplantation such as pretreatment with pro-survival factors and/or encapsulation methods could increase the survival following transplantation.

Taken together, our data provide an efficient strategy for large-scale selection of highly enriched human ISL1+ cardiac progenitors. These cells can be employed for translational applications in cardiac repair, as well as in developmental and disease-related studies. Our approach establishes a template for systematic characterization of various cardiac progenitor populations and dissection of their developmental and regenerative potential.

EXPERIMENTAL PROCEDURES

Culture of Undifferentiated Human ESCs

Adherent colonies of hESC line H9 (WA-09), hESC line Royan H5 and derivatives (rH5-ISL1-Hygro), as well as two independent hiPSC lines (hiPSC1, bj-iPSC1) were maintained on mouse embryonic fibroblasts in knockout serum replacement (KOSR; Invitrogen, #10828-028) containing hESC medium as described previously (Fonoudi et al., 2013).

Generation of ISL1-Hygro hESCs

The hygromycin resistance gene was PCR amplified and subcloned into pBlue-TOPO vector (Life Technologies, #K4831-01). To generate the ISL1-based selection construct, we PCR amplified a 4.1-kb fragment of human ISL1 promoter from human genomic DNA using the Expand Long Template PCR System (Roche, #11681834001). The amplified fragment was cloned in the multiple cloning site of the pBlue-TOPO vector containing the hygromycin resistance fragment using AflII and BglII digestion. The ISL1-Hygro construct was sequenced for validation. To generate the ISL1-Hygro hESC line, we plated and transfected single cells with the construct using Fugene 6 (Promega, #E2693) according to the manufacturer's instructions. The cells were cultured in G418 (Sigma, #A1720)-containing medium for 7 days and resistant colonies were selected for expansion and follow-up validations.

Cardiac Induction

hESCs were plated on Matrigel-coated dishes (10^5 cells/cm^2) in hESC medium containing 100 ng/mL fibroblast growth factor 2 (R&D Systems, #233-FB-001MG/CF). Differentiation was initiated in RPMI-1640 medium (Gibco, #51800-035) supplemented with 2% B27 without vitamin A (Gibco, #12587-010), 2 mM L-glutamine (Gibco, #25030-024), 1 mM nonessential amino acids (Gibco, #11140-035), 1× penicillin/streptomycin (Gibco, #15070-063), and 0.1 mM β-mercaptoethanol (Sigma-Aldrich, #M7522), and containing activin A (100 ng/mL, R&D, #338-AC-050) for 1 day and BMP4 (10 ng/mL, R&D, #314-BP-010) from days 2–5.

Enrichment of ISL1+ cells was accomplished by treatment with hygromycin (10 μM) from day 5 through day 8. The differentiated cells (ISL1+ and ISL+/−) were harvested for protein purification on day 8.

Multi-electrode Array

Extracellular recordings were performed with an MEA data-acquisition system (Multi Channel Systems, Reutlingen, Germany). The MEA plates contained a matrix of 60 titanium nitride electrodes (30 μm in diameter) with an inter-electrode distance of 200 μm. The signal recorded with one of the extracellular electrodes reflects local changes of the membrane potential. The MEA plates were sterilized and coated with polyornithine/laminin/fibronectin. Standard measurements were acquired at 5 kHz (at 37°C). Recordings were performed 48 hr after plating, for 100 s at baseline, and at 5 min after 100 nM isoprenaline. The parameters including filed potential duration (ms), peak amplitude (μV) inter-spike interval duration (ms), and beating rate (beats/min) were analyzed using AxoScope software (Molecular Devices) and CardioMDA.

Fluorescence-Activated Cell Sorting and Immunofluorescence Analysis

For immunofluorescence, cells were washed three times with PBS solution and fixed in 4% paraformaldehyde (Sigma-Aldrich, #P6148) for 20 min, then blocked and permeabilized using 0.3% (v/v) PBS/Triton X-100 and 5% heat-inactivated horse serum for 20 min at room temperature. The cells were then incubated overnight at 4°C with the appropriate primary antibodies and stained with fluorophore-conjugated secondary antibody at room temperature for 1 hr before imaging. For fluorescence-activated cell sorting analysis, cells were dissociated using Accutase (Innovative Cell Technologies, #AT104) treatment for 5 min and fixed and permeabilized using BD Cytofix/Cytoperm solution (Becton Dickinson, #554722) for 30 min at 4°C. After washing twice with PBS, the final pellet was resuspended in 200 μL of BD Perm/Wash buffer (Becton Dickinson, #554723) plus 5% horse serum and incubated for 30 min on ice. The cells were then stained with primary (overnight at 4°C) and secondary (1 hr at 4°C) antibodies and analyzed using Flowjo 8.7 software (Tree Star). A list of primary antibodies and their working dilutions is provided in Supplemental Experimental Procedures.

Gene Expression Analysis

For RNA sequencing, total RNA was extracted using the RNeasy Mini Kit (Qiagen, #74104) according to the manufacturer's protocol. For qRT-PCR assay, 2 μg of total RNA was reverse transcribed to cDNA using RevertAid First Strand cDNA Synthesis Kit (Fermentas, #K1621). qRT-PCR reactions used SYBRPremix Ex Taq II (Takara Bio, #RR081Q). Each data point represents three independent biological replicates.

Protein Separation

Extracted proteins from each sample (150 μg) were fractionated on a 10% Bis-Tris polyacrylamide gels. After staining and washing, each lane was cut into 16 equal pieces from top to bottom, with each piece further sliced into smaller pieces and transferred to a 96-well plate. Gel pieces were briefly washed with 100 mM NH_4HCO_3 and then three times with acetonitrile (can) (50%)/100 mM NH_4HCO_3 (50%), before dehydration with 100% ACN (5 min). Samples were then air dried, reduced with 10 mM DTT/50 mM NH_4HCO_3 for 1 hr at 37°C, and alkylated with 50 mM iodoacetamide/50 mM NH_4HCO_3 for 1 hr at room temperature in darkness. Samples were then digested with 20 μL of trypsin (12.5 ng/mL in 50 mM NH_4HCO_3) for 30 min on ice and at 37°C overnight. Resultant peptides were extracted twice with 50 μL of 50% ACN/2% formic acid, dried, vacuum centrifuged, and reconstituted to 10 μL with 2% formic acid.

Nanoflow Liquid Chromatography-Tandem Mass Spectrometry

Extracted SDS-PAGE gel tryptic digests were analyzed by nanoflow liquid chromatography-tandem mass spectrometry using an LTQ-XL linear ion-trap mass spectrometer (Thermo, San Jose, CA). Reversed-phase chromatography columns were packed to approximately 7 cm length in 100-μm internal diameter tubing using 100 Å, 5 μM Zorbax C18 resin (Agilent Technologies, Santa Clara, CA) in a fused silica capillary with an integrated electrospray tip. An electrospray voltage of 1.8 kV was supplied via a liquid junction upstream of the C18 column. Injection of samples onto the C18 columns was performed using a Surveyor autosampler (Thermo). Each sample loaded onto the C18 column was subjected to an initial wash with buffer A (5% [v/v] ACN, 0.1% [v/v] formic acid) for 10 min at 1 μL/min. Peptides were subsequently eluted with 0%–50% buffer B (95% [v/v] ACN, 0.1% [v/v] formic acid) over 58 min at 500 nL/min, followed by 50%–95% buffer B over 5 min at 500 nL/min, with the eluent directed into the nanospray ionization source of the mass spectrometer and scanned over the range of 400–1,500 atomic mass units. Tandem mass spectrometry of the top six most intense precursor ions at 35% normalization collision energy was performed using Xcalibur software (version 2.06; Thermo). Normalized spectral abundance factor values were calculated for each reproducibly identified protein as previously described (Zybailov et al., 2006). Proteins that were present in all three biological replicates with a summed spectral count of at least 6 were considered to be reproducibly identified and were included in the final dataset. Specific details on statistical analysis are provided in Supplemental Experimental Procedures.

Western Blot Analysis

Proteins were separated by 12% SDS-PAGE electrophoresis at 100 V for 2 hr using a Mini-PROTEAN 3 electrophoresis cell (Bio-Rad) and transferred to a PVDF membrane by wet blotting (Bio-Rad). Membranes were blocked for 1 hr with 5% BSA and incubated for 1.5 hr at room temperature with appropriate primary antibodies. At the end of the incubation period, membranes were rinsed and incubated with anti-rabbit secondary antibody (Sigma-Aldrich, #A0545) conjugated with horseradish peroxidase. Blots were visualized with ECL substrate (GE) with a densitometer (GS-800, Bio-Rad).

Cell Transplantation in Myocardial Infarction Model

Thirty male Sprague-Dawley rats weighing 290–330 g (8–9 weeks of age) were used in this study. The rats were intubated and ventilated with a volume-cycled small-animal ventilator (Harvard Apparatus). Anesthesia was maintained during the operation with aspiration of 5% isoflurane. The chest was opened and once the LAD was identified, it was ligated by 6-0 polypropylene. After ligation, $ALCAM^+$, $ALCAM^-$, or $ALCAM^{+/-}$ cells were injected into the border zone surrounding the infarct area anteriorly and laterally (5×10^5) in three places with a 10-μL Hamilton syringe. The muscle layer of thorax and skin were closed and the rats were allowed to recover. A sham-operated group of animals underwent the same experimental procedure of chest surgery without LAD ligation and cell transplantation. To prevent graft rejection, we treated rats that received cell transplantation with cyclosporine A (10 mg/kg/day). All experimental procedures were performed in accordance with the Institutional Guidelines for Animal Experiments (AAALAC of Gachon University LCDI) and IRB approval (# LCDI-2014-0020). Specific details on evaluation of infarct size, TUNEL assay, immunostaining, immunohistoenzymic 3,3′-diaminobenzidine staining, and cardiac MRI are provided in Supplemental Experimental Procedures.

Microarray Analysis

mRNA expression profiles of H9 hESCs, $ALCAM^-$, $ALCAM^{-/+}$, and $ALCAM^+$ cells were generated using the Agilent-039494 *Human*

8 × 60k chip, which includes 62,976 probes corresponding to 21,755 annotated genes (Agilent). Under each condition gene expression profiling was performed, according to the manufacturer's instructions, on two biological replicates obtained from independent cell cultures. Total RNA was extracted, and the integrity of the total RNA was analyzed using an Agilent 2100 Bioanalyzer. RNA integrity numbers for all the samples were larger than 8. *In vitro* transcription was then performed to generate cRNA, which was hybridized onto each array. The array was scanned using a SureScan Microarray Scanner (Agilent).

The $\log_2$ intensities of the probes from the arrays were normalized using quantile normalization methods (Bolstad et al., 2003). To identify DEGs, we performed an integrative statistical hypothesis test as previously described (Chae et al., 2013). In brief, for each gene we calculated a T-statistic value using Student's t test and also a $\log_2$-median-ratio in each comparison. We then estimated empirical distributions of T statistics and $\log_2$-median-ratio for the null hypothesis (i.e., the genes are not differentially expressed) by performing all possible combinations of random permutations of samples. Using the estimated empirical distributions, we computed adjusted p values for the t test and $\log_2$-median-ratio test for each gene and then combined these p values using Stouffer's method (Hwang et al., 2005). Finally, we identified DEGs as the genes with combined p values of ≤ 0.05 and absolute $\log_2$-median-ratios of ≥ 1 (2-fold change). The gene expression dataset was deposited in the GEO database under the accession number GEO: GSE109339.

Densitometry and Statistical Analysis

The densitometric intensity of each immunoreactive band was determined using Image-Pro gel digitizing software. All data shown in this study represent results from at least three independent experiments. Statistical analyses were performed using the Student's t test, and a p value of less than 0.05 was considered significant (*$p < 0.1$, **$p < 0.01$, ***$p < 0.001$ in figures).

SUPPLEMENTAL INFORMATION

Supplemental Information includes Supplemental Experimental Procedures, five figures, three tables, and two movies and can be found with this article online at https://doi.org/10.1016/j.stemcr.2018.01.037.

AUTHOR CONTRIBUTIONS

Z.G., design and conception of the study, maintenance, directed differentiation of human PSCs, cellular/molecular assays, electrophysiology, proteomics data analysis, and writing of manuscript; F.F., design and conception of the study, writing of manuscript, maintenance, directing differentiation, and genetic manipulation of human PSCs; M.M. and P.A.H., mass spectrometry, proteomics analysis, and writing of manuscript; S.C. and D.H., microarray expression profiling and data analysis; D.B., J.L., and K.B., establishing AMI model in rats, transplantation of cardiac progenitors, and histological analysis; M.S.T., qRT-PCR expression analysis; S.T., protein sample preparation for proteomics; S.M., western blotting; P.S. and H.F., optimization of differentiation conditions; H.B. and N.A., study design and data interpretation; T.E., data interpretation and writing of manuscript; B.L., design and execution of *in vivo* experiments in AMI rat models; G.H.S., design and conception of the study, data interpretation, and writing of manuscript.

ACKNOWLEDGMENTS

We would like to acknowledge members of the Department of Stem Cells and Developmental Biology laboratories for their helpful suggestions and critical reading of the manuscript. This study was funded by grants provided by the Royan Institute, the Iranian Council of Stem Cell Research and Technology, and the Korean National Research Foundation (2017M3A9B402814) and was supported by Chungcheongbuk-do.

Received: April 14, 2017
Revised: January 29, 2018
Accepted: January 30, 2018
Published: March 1, 2018

REFERENCES

Ardehali, R., Ali, S.R., Inlay, M.A., Abilez, O.J., Chen, M.Q., Blauwkamp, T.A., Yazawa, M., Gong, Y., Nusse, R., Drukker, M., et al. (2013). Prospective isolation of human embryonic stem cell-derived cardiovascular progenitors that integrate into human fetal heart tissue. Proc. Natl. Acad. Sci. USA *110*, 3405–3410.

Bolstad, B.M., Irizarry, R.A., Astrand, M., and Speed, T.P. (2003). A comparison of normalization methods for high density oligonucleotide array data based on variance and bias. Bioinformatics *19*, 185–193.

Bu, L., Jiang, X., Martin-Puig, S., Caron, L., Zhu, S., Shao, Y., Roberts, D.J., Huang, P.L., Domian, I.J., and Chien, K.R. (2009). Human ISL1 heart progenitors generate diverse multipotent cardiovascular cell lineages. Nature *460*, 113–117.

Buckingham, M., Meilhac, S., and Zaffran, S. (2005). Building the mammalian heart from two sources of myocardial cells. Nat. Rev. Genet. *6*, 826–835.

Cai, C.L., Liang, X., Shi, Y., Chu, P.H., Pfaff, S.L., Chen, J., and Evans, S. (2003). Isl1 identifies a cardiac progenitor population that proliferates prior to differentiation and contributes a majority of cells to the heart. Dev. Cell *5*, 877–889.

Chae, S., Ahn, B.Y., Byun, K., Cho, Y.M., Yu, M.H., Lee, B., Hwang, D., and Park, K.S. (2013). A systems approach for decoding mitochondrial retrograde signaling pathways. Sci. Signal. *6*, rs4.

Dodou, E., Verzi, M.P., Anderson, J.P., Xu, S.M., and Black, B.L. (2004). Mef2c is a direct transcriptional target of ISL1 and GATA factors in the anterior heart field during mouse embryonic development. Development *131*, 3931–3942.

Drukker, M., Tang, C., Ardehali, R., Rinkevich, Y., Seita, J., Lee, A.S., Mosley, A.R., Weissman, I.L., and Soen, Y. (2012). Isolation of primitive endoderm, mesoderm, vascular endothelial and trophoblast progenitors from human pluripotent stem cells. Nat. Biotechnol. *30*, 531–542.

Dubois, N.C., Craft, A.M., Sharma, P., Elliott, D.A., Stanley, E.G., Elefanty, A.G., Gramolini, A., and Keller, G. (2011). SIRPA is a specific cell-surface marker for isolating cardiomyocytes derived from human pluripotent stem cells. Nat. Biotechnol. *29*, 1011–1018.

Fernandes, S., Chong, J.J.H., Paige, S.L., Iwata, M., Torok-Storb, B., Keller, G., Reinecke, H., and Murry, Charles E. (2015). Comparison of human embryonic stem cell-derived cardiomyocytes, cardiovascular progenitors, and bone marrow mononuclear cells for cardiac repair. Stem Cell Reports *5*, 753–762.

Fonoudi, H., Yeganeh, M., Fattahi, F., Ghazizadeh, Z., Rassouli, H., Alikhani, M., Mojarad, B.A., Baharvand, H., Salekdeh, G.H., and Aghdami, N. (2013). ISL1 protein transduction promotes cardiomyocyte differentiation from human embryonic stem cells. PLoS One *8*, e55577.

Hwang, D., Rust, A.G., Ramsey, S., Smith, J.J., Leslie, D.M., Weston, A.D., de Atauri, P., Aitchison, J.D., Hood, L., Siegel, A.F., et al. (2005). A data integration methodology for systems biology. Proc. Natl. Acad. Sci. USA *102*, 17296–17301.

Kwon, C., Qian, L., Cheng, P., Nigam, V., Arnold, J., and Srivastava, D. (2009). A regulatory pathway involving Notch1/beta-catenin/Isl1 determines cardiac progenitor cell fate. Nat. Cell Biol. *11*, 951–957.

Laflamme, M.A., Chen, K.Y., Naumova, A.V., Muskheli, V., Fugate, J.A., Dupras, S.K., Reinecke, H., Xu, C., Hassanipour, M., Police, S., et al. (2007). Cardiomyocytes derived from human embryonic stem cells in pro-survival factors enhance function of infarcted rat hearts. Nat. Biotechnol. *25*, 1015–1024.

Laugwitz, K.L., Moretti, A., Lam, J., Gruber, P., Chen, Y., Woodard, S., Lin, L.Z., Cai, C.L., Lu, M.M., Reth, M., et al. (2005). Postnatal isl1+ cardioblasts enter fully differentiated cardiomyocyte lineages. Nature *433*, 647–653.

Liang, X., Zhang, Q., Cattaneo, P., Zhuang, S., Gong, X., Spann, N.J., Jiang, C., Cao, X., Zhao, X., Zhang, X., et al. (2015). Transcription factor ISL1 is essential for pacemaker development and function. J. Clin. Invest. *125*, 3256–3268.

Lin, B., Kim, J., Li, Y., Pan, H., Carvajal-Vergara, X., Salama, G., Cheng, T., Li, Y., Lo, C.W., and Yang, L. (2012). High-purity enrichment of functional cardiovascular cells from human iPS cells. Cardiovasc. Res. *95*, 327–335.

Scavone, A., Capilupo, D., Mazzocchi, N., Crespi, A., Zoia, S., Campostrini, G., Bucchi, A., Milanesi, R., Baruscotti, M., Benedetti, S., et al. (2013). Embryonic stem cell-derived CD166+ precursors develop into fully functional sinoatrial-like cells. Circ. Res. *113*, 389–398.

Sun, Y., Liang, X., Najafi, N., Cass, M., Lin, L., Cai, C.L., Chen, J., and Evans, S.M. (2007). Islet 1 is expressed in distinct cardiovascular lineages, including pacemaker and coronary vascular cells. Dev. Biol. *304*, 286–296.

Wu, S.M., Chien, K.R., and Mummery, C. (2008). Origins and fates of cardiovascular progenitor cells. Cell *132*, 537–543.

Zhu, W.H., MacIntyre, A., and Nicosia, R.F. (2002). Regulation of angiogenesis by vascular endothelial growth factor and angiopoietin-1 in the rat aorta model: distinct temporal patterns of intracellular signaling correlate with induction of angiogenic sprouting. Am. J. Pathol. *161*, 823–830.

Zybailov, B., Mosley, A.L., Sardiu, M.E., Coleman, M.K., Florens, L., and Washburn, M.P. (2006). Statistical analysis of membrane proteome expression changes in Saccharomyces cerevisiae. J. Proteome Res. *5*, 2339–2347.